Energy Transfer from a Surface-Bound Arene to the Gold Core in ω-Fluorenyl-Alkane-1-Thiolate Monolayer-Protected Gold Clusters

Tao Gu, James K. Whitesell, and Marye Anne Fox*

Department of Chemistry, North Carolina State University, Raleigh, North Carolina 27695-8204

Received October 2, 2002. Revised Manuscript Received January 17, 2003

9-(9-Fluorenyl)-nonane-1-thiolate and 12-(9-fluorenyl)-dodecane-1-thiolate (fluorenyl-alkane-1-thiolates) monolayer-protected gold clusters (Au-MPCs) have been prepared by place exchange of fluorenyl-alkane-1-thiol with alkane-1-thiolate Au-MPCs. The structures of these composites were established by TEM, elemental analysis, and ^{1}H NMR spectroscopy. Changes in optical and physical properties caused by attachment of the fluorenyl groups to the gold nanoparticles were studied by absorption, Fourier transform infrared, and fluorescence spectroscopies. Emission from the end-attached fluorenyl groups is substantially quenched upon attachment to a gold cluster so that less than 5% of emission intensity from an optically matched solution of the analogous freely dissolved fluorene and alkane-1-thiolate Au-MPCs is retained in the fluorenyl-alkane-1-thiolate Au-MPCs. Nanosecond flash photolysis shows that intersystem crossing (from the fluorenyl singlet to the corresponding triplet) was suppressed because energy transfer was much faster. No direct evidence of electron transfer from the excited fluorenyl group to the gold cluster could be observed, implying that electronic coupling through energy transfer accounts for most of the observed emission quenching and suppressed intersystem crossing.

Introduction

Scientific interest in nanotechnology[1a−e] and in the optical and electronic properties of nanoarrays[1f,g] derives from a desire for a full understanding of how complex organic aggregates and organic−inorganic composite assemblies can be constructed from simple molecular precursors. It is also important to establish how the physical properties of the resulting material vary with the size of the component array.[1] Current theories fail to provide a convincing predictive model of how the aggregated properties of integrated chemical systems differ from those in which the individual molecular components are randomly dispersed.[1h−p] Advances in this field thus require that architecturally defined arrays be prepared and that a clear correlation of structure with photochemical reactivity be explored.

Nanoparticles produced on a Au core with a diameter of several nanometers can be synthesized with a dense monolayer coating of alkane-1-thiolate.[2a] The method described by Brust involves displacement of a phase-transfer capping reagent by one or more saturated alkane thiolates.[2a] Murray and co-workers have described efficient strategies for functionalizing MPCs by ligand place exchange (to form poly-homo- and -hetero-functionalized MPCs), nucleophilic substitution, and ester and amide coupling.[2−7] The resulting MPCs are large, complex species with multiple functionalities, roughly spherically organized around a central metallic core. The spatial arrangement of the resulting MPCs is thus reminiscent of shell−core dendrimers studied over the last several years by our group.[8,9] However, whereas

(1) (a) Fox, M. A. *Acc. Chem. Res.* **1999**, *32*, 201. (b) Whitesides, G. M.; Mathias J. P.; Seto, C. T. *Science* **1991**, *254*, 1312. (c) Wang, D.; Thomas, S. G.; Wang, K. L.; Xia, Y.; Whitesides, G. M. *Appl. Phys. Lett.* **1997**, *70*, 1593. (d) Choi, I. S.; Bowden, N.; Whitesides, G. M. *J. Am. Chem. Soc.* **1999**, *121*, 1754. (e) Shipway, A. N.; Lahav, M.; Willner, I. *Adv. Mater.* **2000**, *12*, 993. (f) Alivisatos, A. P.; Johnsson, K. P.; Peng, X.; Wilson, T. E.; Loweth, C. J.; Bruchez, M. P., Jr.; Schultz, P. G. *Nature* **1996**, *382*, 609. (g) Weller, H. *Angew. Chem., Int. Ed.* **1998**, *37*, 1658. (h) Li, F.; Yang, S. I.; Ciringh, Y.; Seth, J.; Martin, C. H.; Singh, D. L.; Kim, D.; Birge, R. R.; Bocian, D. F.; Holten, D.; Lindsey, J. S. *J. Am. Chem. Soc.* **1998**, *120*, 10001. (i) Kuciauskas, D.; Liddell, P. A.; Lin, S.; Johnson, T. E.; Weghorn, S. J.; Lindsey, J. S.; Moore, A. L.; Moore, T. A.; Gust, D. *J. Am. Chem. Soc.* **1999**, *121*, 8604. (j) Gust, D.; Moore, T. A. *Acc. Chem. Res.* **1993**, *26*, 198. (k) Wasielewski, M. R. *Chem. Rev.* **1992**, *92*, 435. (l) Fox, M. A.; Thompson, H. K. *Macromolecules* **1997**, *30*, 7391. (m) Lu, L.; Lachicotte, R. J.; Penner, T. L.; Perlstein, J.; Whitten, D. G. *J. Am. Chem. Soc.* **1999**, *121*, 8146. (n) O'Regan, B.; Grätzel, M. *Nature* **1991**, *353*, 737. (o) Bonhote, P.; Moser, J.-E.; Humphry-Baker, R.; Vlachopoulos, N.; Zakeeruddin, S. M.; Walder, L.; Grätzel, M. *J. Am. Chem. Soc.* **1999**, *121*, 1324. (p) Lamont, R. E.; Ducker, W. A. *J. Am. Chem. Soc.* **1998**, *120*, 7602.

(2) (a) Brust, M.; Walker, M.; Bethell, D.; Schiffrin, D. J.; Whyman, R. *J. Chem. Soc., Chem. Commun.* **1994**, 801. (b) Templeton, A. C.; Wuelfing, W. P.; Murray, R. W. *Acc. Chem. Res.* **2000**, *33*, 27.

(3) Newkome, G. R.; Moorefield, C. N.; Vögtle, F. *Dendritic Molecules: Concepts, Synthesis, Prospectives*; VCH: New York, 1996.

(4) Templeton, A. C.; Hosteter, M. J.; Kraft, C. T.; Murray, R. W. *J. Am. Chem. Soc.* **1998**, *120*, 1906.

(5) Hostetler, M. J.; Green, S. J.; Stokes, J. J.; Murray, R. W. *J. Am. Chem. Soc.* **1996**, *118*, 4212.

(6) Ingram, R. S.; Hostetler, M. J.; Murray, R. W. *J. Am. Chem. Soc.* **1997**, *119*, 9175.

(7) Templeton, A. C.; Hostetler, M. J.; Warmoth, E. K.; Chen, S.; Hartshorn, C. M.; Krishnamurthy, V. M.; Forbes, M. D. E.; Murray, R. W. *J. Am. Chem. Soc.* **1998**, *120*, 4845.

(8) Ghaddar, T. H.; Wishart, J. F.; Thompson, D. W.; Whitesell, J. K.; Fox, M. A. *J. Am. Chem. Soc.* **2002**, *124*, 8285.

(9) Ghaddar, T. H.; Wishart, J. F.; Kirby, J. P.; Whitesell, J. K.; Fox, M. A. *J. Am. Chem. Soc.* **2001**, *123*, 12832.

10.1021/cm0209867 CCC: $25.00
Published on Web 02/28/2003

Scheme 1. FlC_9S−Au-MPC Was Prepared by Place Exchange of C_9S−Au-MPC and FlC_9SH

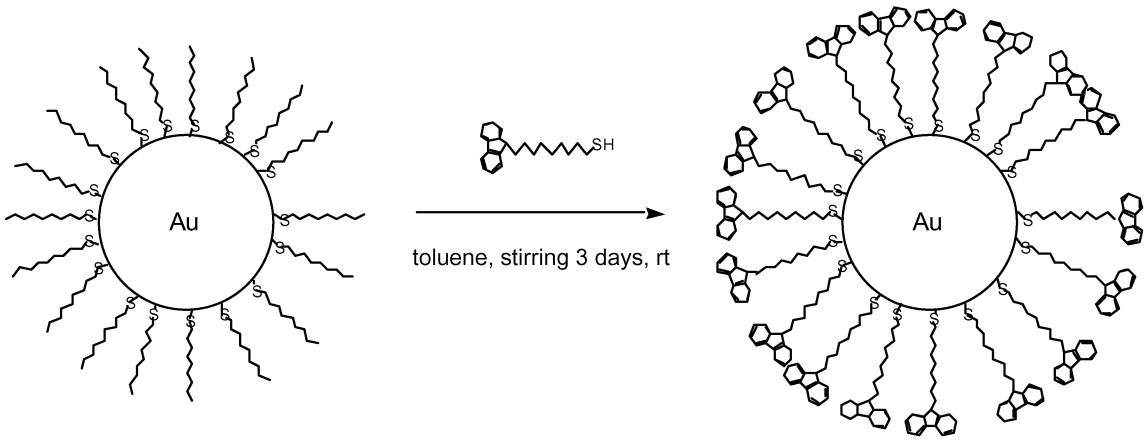

C_9S-Au-MPC $F1C_9S$-Au-MPC

a dendrimer with an end-functionalized group is sometimes more densely packed at its perimeter than at its core, MPCs are "soft objects with hard cores".[2]

Fluorophore-modified gold nanoclusters are important as possible biological sensors and in optoelectronic devices.[10−12] The factors that influence the efficiency of emission from electronically excited groups bound at the outer edge of a MPC with a metal-like core, however, are not well-understood. Fluorophores bound directly to a bulk gold surface are often strongly coupled to the metal support via energy or electron transfer and their emission is thus at least partially quenched. For example, Murray has reported distance-dependent energy transfer from an end-substituted excited dansyl label bound to a metal-like core in a gold MPC.[13] Kamat and co-workers report that direct electron transfer between a gold nanoparticle and a surface-bound pyrene can be induced by pulsed laser irradiation.[14] They also found efficient energy transfer between a gold nanocore and an array of appended fullerene moieties.[15] Imahori et al. report that binding porphyrins to the surface of a MPC suppresses complications from undesirable electronic coupling relative to the corresponding self-assembled monolayer.[16] Our own group has found that photochemical reactivity is retained in self-assembled monolayers on metals. For example, 6-thiohexyl-3-nitro-4-(4′-stilbenoxymethyl)-benzoate and analogous derivatives of azobenzene or stilbene, when bound as monolayers to a planar gold surface, exhibit efficient trans-to-cis photoisomerization and photodimerization.[17] With the latter compounds, the efficiency of photodimerization is lower when these chromophores are bound to gold clusters than when attached to a planar surface.

In this paper, we report high-density loading of end-bound fluorenyl groups on 2.2-nm gold clusters by place exchange of alkane-1-thiolate Au-MPCs by fluorene-functionalized alkane thiols (Scheme 1, where the C_9 thiol is illustrated). Upon exhaustive exchange, the end-functionalized fluorenyl thiols become densely packed at the periphery of the organic layer bound to the core gold cluster. Changes in optical and physical properties caused by chromophore aggregation in the Au-MPC were studied. Fluorescence emission and nanosecond flash photolysis were used to monitor the efficiency of competing excited states processes, including intersystem crossing. These techniques were proven recently to be helpful in the full physical description of these composite systems.[18]

Experimental Section

All reagents and solvents were reagent-grade and were used without further purification. ^{1}H NMR spectra were recorded on a Varian 300 or 400 MHz instrument with solvent peaks as reference. Absorption spectra were recorded on a Shimadzu PC-3101PC instrument. Transmission Fourier transform infrared (FTIR) spectra were acquired on a Nicolet 510P spectrometer. A solid sample on a KBr crystal was prepared by evaporating a dilute solution of the nanoparticles from dichloromethane. Typically, 1024 scans at a resolution of about 4 cm^{-1} were collected. Steady-state fluorescence spectra were measured on a PTI Quanta Master model C-60/2000 spectrofluorometer.

The 9-(9-fluorenyl)-nonane-1-bromide and 12-(9-fluorenyl)-dodecane-1-bromide were prepared using a modification of the Cedheim and Eberson procedure.[19] The corresponding 9-(9-fluorenyl)-nonane-1-thiol and 12-(9-fluorenyl)-dodecane-1-thiol were prepared in high yield from each of the corresponding bromides by a previously reported displacement reaction.[20]

Preparation of Au-MPCs. Nonane-1-thiol and dodecane-1-thiol capped gold clusters were prepared by a modification of Murray's procedure.[21] A molar ratio of thiol:$HAuCl_4 \cdot 3H_2O$:tetraoctylammonium bromide:$NaBH_4$ of 2:1:2.5:10 produced a capped gold cluster of about 2.2-nm diameter. To a vigorously stirred solution of 350 mg of tetraoctylammonium bromide (2.5 equiv) in 12 mL of toluene was added 100 mg of $HAuCl_4 \cdot 3H_2O$

(10) Chen, S.; Ingram, R. S.; Hostetler, M. J.; Pietron, J. J.; Murray, R. W.; Schaaff, T. G.; Khoury, J. T.; Alvarez, M. M.; Whetten, R. L. *Science* **1998**, *280*, 2098.
(11) Hickman, J. J.; Ofer, D.; Laibinis, P. E.; Whitesides, G. M.; Wrighton, M. S. *Science* **1991**, *252*, 688.
(12) Elghanian, R.; Storhoff, J. J.; Mucic, R. C.; Letsinger, R. L.; Mirkin, C. A. *Science* **1997**, *277*, 1078.
(13) Aguila, A.; Murray, R. W. *Langmuir* **2000**, *16*, 5949.
(14) Ipe, B. I.; Thomas, K. G.; Barazzouk, S.; Hotchandani, S.; Kamat, P. V. *J. Phys. Chem. B* **2002**, *106*, 18.
(15) Sudeep, P. K.; Ipe, B. I.; Thomas, K. G.; George, M. V.; Barazzouk, S.; Hotchandani, S.; Kamat, P. V. *Nano Lett.* **2002**, *2*, 29.
(16) Imahori, H.; Arimura, M.; Hanada, T.; Nishimura, Y.; Yamazaki, I.; Sakata, Y.; Fukuzumi, S. *J. Am. Chem. Soc.* **2001**, *123*, 335.
(17) (a) Hu, J.; Zhang, J.; Liu, F.; Kittredge, K.; Whitesell, J. K.; Fox, M. A. *J. Am. Chem. Soc.* **2001**, *123*, 1464. (b) Zhang, J.; Whitesell, J. K.; Fox, M. A. *Chem. Mater.* **2001**, *13*, 2323.
(18) Dulkeith, E.; Morteani, A. C.; Niedereichholz, T.; Klar, T. A.; Feldmann, J.; Levi, S. A.; van Veggel, F. C. J. M.; Reinhoudt, D. N.; Möller, M.; Gittins, D. I. *Phys. Rev. Lett.* **2002**, *89*, 203002.
(19) Cedheim, L.; Eberson, L. *Synthesis* **1973**, 159.
(20) Hu, J.; Fox, M. A. *J. Org. Chem.* **1999**, *64*, 4959.
(21) Hostetler, M. J.; Stokes, J. J.; Murray, R. W. *Langmuir* **1996**, *12*, 3604.

Table 1. Composition of Alkane-1-thiolate Au-MPCs

sample name	core size by TEM (nm)	number of Au atoms[a]	number of Au atoms on the surface[a]	elemental analysis (C/H/S/organic)	number of organic chain	fractional surface coverage
C_9S−Au-MPC	2.2 ± 0.7	323	159	15.07/2.72/4.33/22.1%	113	71%
$C_{12}S$−Au-MPC	2.2 ± 0.6	323	159	19.87/3.43/4.36/27.7%	120	75%

[a] Calculation of the number of Au atoms on the surface was based on the assumption that the average MPC core has a closed-shell structure and a spherical core. A detailed calculation has been discussed in the text.

Table 2. Composition of Fluorenyl-Labeled Au-MPCs

sample name	feed ratio: cluster ligand/thiol[a]	percentage of initial thiol exchanged by incoming thiol[b]	composition[c]
C_9S−Au-MPC			$Au_{323}(C_9S)_{113}$
$C_{12}S$−Au-MPC			$Au_{323}(C_{12}S)_{120}$
FlC_9S−Au-MPC	1/2	100	$Au_{323}(FlC_9S)_{113}$
FlC_9S/C_9S−Au-MPC	1/1	71	$Au_{323}(FlC_9S)_{80}(C_9S)_{33}$
FlC_9S/C_9S−Au-MPC	1/0.4	48	$Au_{323}(FlC_9S)_{54}(C_9S)_{59}$
$FlC_{12}S/C_9S$−Au-MPC	1/2	81	$Au_{323}(FlC_{12}S)_{92}(C_9S)_{21}$
$FlC_9S/C_{12}S$−Au-MPC	1/2	84	$Au_{323}(FlC_9S)_{101}(C_{12}S)_{19}$
$FlC_{12}S/C_{12}S$−Au-MPC	1/2	62	$Au_{323}(FlC_{12}S)_{74}(C_{12}S)_{46}$

[a] Feed ratio of initial protecting alkane-1-thiolate ligands to incoming fluorenyl-alkane-1-thiol. [b] The percentage of the initial protecting alkane-1-thiolate ligands exchanged by fluorenyl-alkane-1-thiolate ligands was established by ^{1}H NMR (see Supporting Information). [c] The average composition of alkane-1-thiolate Au-MPC was established by TEM and elemental analysis assuming that the average MPC core has a closed-shell structure and a roughly spherical shape. ^{1}H NMR was then used to measure the ratio of nonexchanged alkane-1-thiolate ligands to exchanged fluorenyl-alkane-1-thiolate ligands. The ratio was converted into number of exchanged ligands, based on the average composition of alkane-1-thiolate MPC. Proton atoms are not shown in the composition.

(1 equiv) in 4 mL of deionized water. The yellow $HAuCl_4 \cdot 3H_2O$ aqueous solution quickly cleared and the toluene phase became orange-red as the $AuCl_4^-$ was phase-transferred. The organic phase was isolated, the desired amount of alkane-1-thiol was added, and the resulting solution was stirred for 20 min at room temperature. Sodium borohydride (96 mg, 10 equiv) in 3 mL of deionized water was added in one aliquot. The very dark organic phase was further stirred at room temperature overnight. The organic phase was collected and the solvent was removed by rotary evaporation. The black product was suspended in 50 mL of ethanol, collected on a glass filtration frit, and washed with copious amounts of ethanol and acetone.

Thiol exchange was accomplished according to the reported procedure.[5] The alkane-1-thiolate gold clusters and fluorenyl-alkane-1-thiol were stirred in toluene solution at room temperature for 3 days, after which solvent was removed under vacuum. The resulting precipitate was washed copiously with ethanol and acetone to remove any unreacted fluorenyl-alkane-1-thiol ligands and displaced alkane-1-thiol before being collected via filtration. ^{1}H NMR was then used to measure the ratio of nonexchanged alkane-1-thiolate ligands to exchanged fluorenyl-alkane-1-thiolate ligands. The ratio was converted into a fraction of exchanged ligands based on the average alkane-1-thiolate gold cluster composition. A series of fluorenyl-alkane-1-thiol capped Au-MPCs was prepared with different alkyl chain lengths (C_9 and C_{12}) and different feed ratios of fluorenyl-alkane-1-thiol (incoming thiolate ligands) and alkane-1-thiol (initial protecting thiolate ligands, see Table 1 and Table 2).

The preparation of gold clusters by the direct reduction of $AuCl_4^-$ with $NaBH_4$ in the presence of 9-(9-fluorenyl)-nonane-1-thiol was accomplished by the same procedure as in the preparation of the alkane-1-thiolate Au-MPCs, except that 9-(9-fluorenyl)-nonane-1-thiol was used in place of alkane-1-thiol. A 100% molar excess of 9-(9-fluorenyl)-nonane-1-thiol over gold was used.

To simplify the description, we use the following abbreviations: nonane-1-thiol (C_9SH), dodecane-1-thiol ($C_{12}SH$), 9-(9-fluorenyl)-nonane-1-thiol (FlC_9SH), 12-(9-fluorenyl)-dodecane-1-thiol ($FlC_{12}SH$), nonane-1-thiolate MPC (C_9S−Au-MPC), dodecane-1-thiolate MPC ($C_{12}S$−Au-MPC), 9-(9-fluorenyl)-nonane-1-thiolate MPC (FlC_9S−Au-MPC), gold clusters protected by a mixed monolayer of alkane-1-thiol and fluorenyl-alkane-1-thiol (FlC_9S/C_9S−Au-MPC, $FlC_9S/C_{12}S$−Au-MPC, $FlC_{12}S/C_9S$−Au-MPC, $FlC_{12}S/C_{12}S$−Au-MPC).

High-Resolution Transmission Electron Microscopy (TEM). TEM studies were performed with a Hitachi HD-2000 STEM (200 keV) spectrometer. TEM samples were prepared by drop casting a solution of the MPCs in toluene, typically at a concentration of 1 mg/mL, onto a grid with 50- or 150-nm silicon nitride membrane windows. Phase-contrast TEM micrographs were typically taken at three different spots of the resulting grid with 500−2000 K magnification. Particle size analysis was then performed by digitizing the micrographs with Scion image software (available at www.scioncorp.com), from which the histograms of the particle size distribution were generated. Twin or particle aggregates were removed manually prior to size measurements.

Nanosecond Flash Photolysis. The fourth harmonic of a Nd:YAG laser (Continuum Surelite III) was used as the excitation source for nanosecond flash photolysis. The detection system consisted of a Xe arc lamp (1 kW, Spectral Energy) and a monochromator (CVI Digikrom 240) with an attached photodetector (Hamamatsu HC120-08 module with a R6358-01 PMT). Signals were digitized with a LeCroy 9350AM oscilloscope for computer analysis. The transient absorption kinetics at each wavelength probed was determined by averaging 5−20 single-shot experiments.

Results and Discussion

Size and Composition of the Au-MPCs. Ligand place exchange was a key step in achieving MPC functionalization by the reaction[22]

$$x(\mathrm{R'SH}) + (\mathrm{RS})_m\mathrm{MPC} \leftrightarrow x(\mathrm{RSH}) + (\mathrm{R'S})_x(\mathrm{RS})_{m-x}\mathrm{MPC} \quad (1)$$

where x, m, and $m-x$ are the numbers of new, original, and nonexchanged ligands, respectively. The new thiolate ligand (R′S) is incorporated into a cluster monolayer by mixing a solution of the thiol (R′SH) and the gold cluster capped by the alkane-1-thiolate (RS)-Au-MPC. The displaced thiolate is dispersed into solution as a thiol (RSH), and the entering R′S group disappears from

(22) Hostetler, M. J.; Templeton, A. C.; Murray, R. W. *Langmuir* **1999**, *15*, 3782.

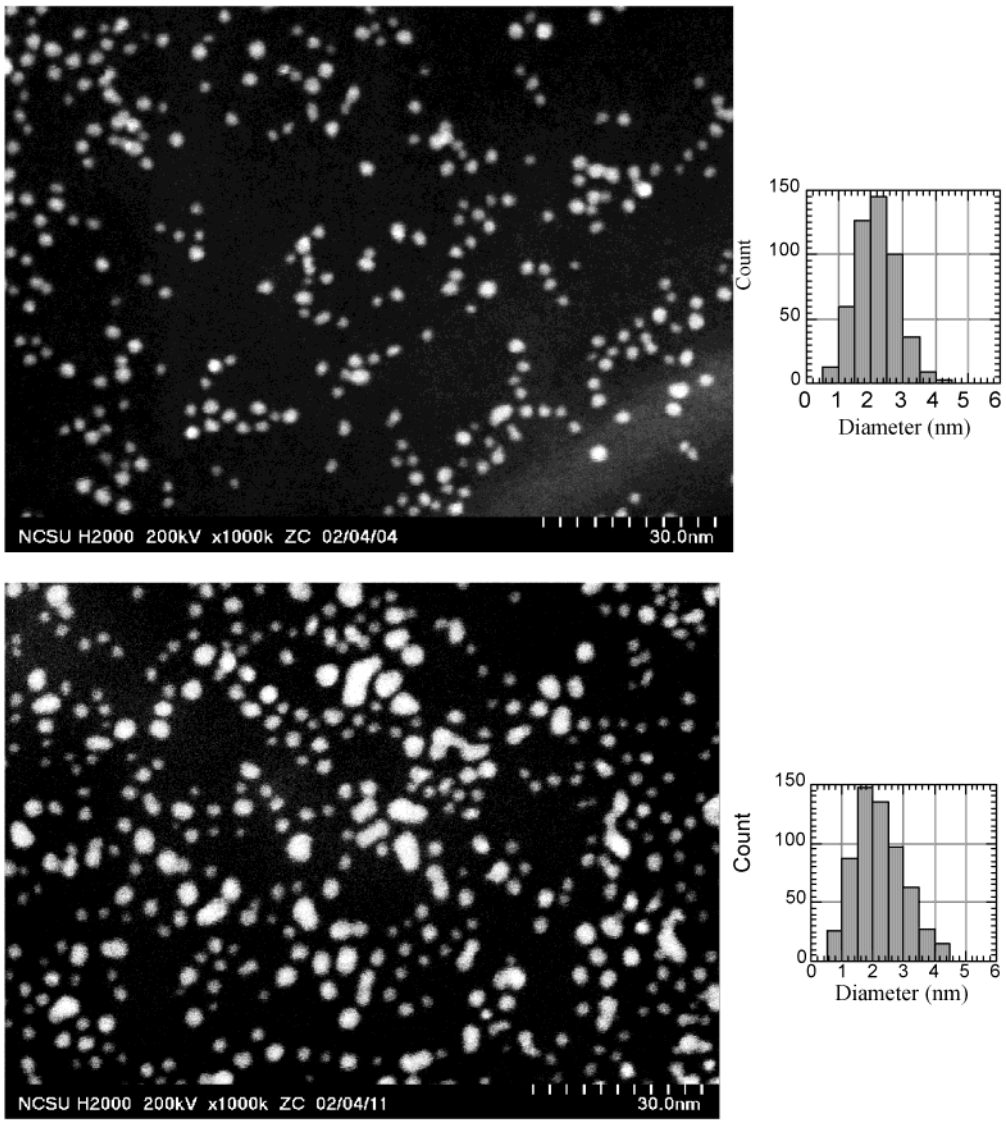

Figure 1. TEM micrographs of C_9S−Au-MPC (bottom, the average diameter is 2.2 nm with the deviation 0.7 nm) and $C_{12}S$−Au-MPC (top, the average diameter is 2.2 nm with the deviation 0.6 nm). The size bars represent 30 nm. Beside the images are the corresponding size distribution histograms.

the R′SH solution population. The rate and equilibrium stoichiometry of ligand place-exchange reactions are controlled by factors that include the solution-phase molar ratio of R′SH to RSH at equilibrium, the relative steric bulk of the two thiols, and their respective chain lengths.[2] A typical MPC contains only a small number of ligands that are bound weakly enough to be lost as disulfides at 100 °C, and ligand loss does not occur at all at room temperature without a displacing ligand, except over long periods of time and with very short alkane-1-thiolate chains (e.g., C_4S−Au-MPC).

In our experiment, place-exchange reactions were used for the preparation of fluorenyl-alkane-1-thiolate Au-MPCs in which C_9SH and $C_{12}SH$ were used as initial protecting thiolate ligands, and fluorenyl-containing thiols with the linker chain lengths of C_9 and C_{12} were used as incoming groups. The fluorophore-labeled gold clusters are stable in the solution and no evidence could be found for room temperature desorption into solution. A reaction time of 3 days produced MPCs that resisted further compositional change over the time period of our additional measurements.

The TEM images in Figure 1 show the cluster sizes and distributions attained by this synthetic route. Neither particle size nor distribution was sensitive to the chain length of the initial capping alkane-1-thiol for C_9SH or $C_{12}SH$. The average formula for a thiol-capped gold MPC, established by TEM,[23,24a] allows calculation of an average core diameter. Assuming that the average MPC core has a closed-shell structure and a spherical core, thermogravimetry gives a value for the organic coating that agrees (within 7%)[24a] with independent elemental analysis.

(23) Hostetler, M. J.; Wingate, J. E.; Zhong, C.-Z.; Harris, J. E.; Vachet, R. W.; Clark, M. R.; Londono, J. D.; Green, S. J.; Stokes, J. J.; Wignall, G. D.; Glish, G. L.; Porter, M. D.; Evans, N. D.; Murray, R. W. *Langmuir* **1998**, *14*, 17.

(24) (a) Terrill, R. H.; Postlethwaite, T. A.; Chen, C.-h.; Poon, C.-D.; Terzis, A.; Chen, A.; Hutchison, J. E.; Clark, M. R.; Wignall, G.; Londono, J. D.; Superfine, R.; Falvo, M.; Johnson, C. S., Jr.; Samulski, E. T.; Murray, R. W. *J. Am. Chem. Soc.* **1995**, *117*, 12537. (b) Chidsey, C. E. D.; Liu, G.-Y.; Rowntree, Y. P.; Scoles, G. *J. Chem. Phys.* **1989**, *91*, 4421. (c) Alves, C. A.; Smith, E. L.; Porter, M. D. *J. Am. Chem. Soc.* **1992**, *114*, 1222. (d) Widrig, C. A.; Alves, C. A.; Porter, M. D. *J. Am. Chem. Soc.* **1991**, *113*, 2805. (e) Strong, L.; Whitesides, G. M. *Langmuir* **1988**, *4*, 546. (f) Chidsey, C. E. D.; Loiacono, D. N. *Langmuir* **1990**, *6*, 682.

Thus, the mean diameter of the gold core in C_9S−Au-MPC was determined by TEM to be 2.2 nm (with a standard deviation $\sigma = 0.7$ nm), yielding an average formula of $Au_{323}(S(CH_2)_9H)_{113}$. A tight-packed spherical model assigns the gold core as a sphere with density ρ_{Au} (the atom density of bulk gold is 58.01 atoms/nm^3) covered with a skin of hexagonally close-packed gold atoms (the number density of surface gold atoms is 13.89 atoms/nm^2).[24a] The radius of the skin is taken as the center of the atoms on the skin (at $R_{CORE} - R_{Au}$, $R_{Au} = 0.145$ nm, crystallographic radius of a gold atom). The spherical model, for this R_{CORE} value, predicts the core of C_9S−Au-MPC to contain 323 Au atoms, of which 159 lie on the surface. From the elemental analysis of the C_9S−Au-MPC (H, 2.72%; C, 15.07%; S, 4.33%) we calculate that the fractional amounts of C, H, and S found in the elemental analysis were in close agreement with the composition of the C_9SH monomer). We calculate that 113 nonane-1-thiolate chains are bound onto the 159 gold atoms present at the surface. The coverage ratio (γ, number of chains of C_9S−Au-MPCs to surface Au atoms) is thus determined as 71%, which is remarkably increased relative to the coverage ratio ($\gamma = 33\%$) reported for sample alkane-1-thiolate SAMs on planar gold. (Helium diffraction, atomic force microscopy, scanning tunneling microscopy, and transmission electron diffraction studies have earlier confirmed that the structure formed by an alkane-1-thiol on Au(111) is commensurate with the underlying gold lattice and is a simple ($\sqrt{3} \times \sqrt{3}$) R 30° overlayer).[24b−f] This may reflect either a small R_{CORE} value, which splays the attached alkane-1-thiol chains outward from one another, relieving steric crowding, and/or the relative reactivity of atoms on the highly curved cluster surface (relative to that of planar gold).[24a] The enhanced packing density in the alkane-1-thiol chains may, in effect, force the elimination of conformational irregularities in the organic layer.

^{1}H NMR spectra of alkane-1-thiolate Au-MPCs exhibit peaks at δ 0.89 and 1.26 ppm, corresponding to the methyl and methylene resonances, respectively. The progress of the place exchange by fluorenyl-alkane-1-thiol displacing alkane-1-thiolate from the Au-MPCs could be followed by ^{1}H NMR spectroscopy by monitoring the appearance of a peak at 3.9 assigned to the CH proton on the fluorenyl ring. The ratio of this peak to those assigned to the methyl and methylene protons gives an approximate surface composition of the exchanged Au-MPCs. The ^{1}H NMR spectra of Au-MPCs are characteristically broadened relative to those of free thiols because of differences in spin−spin relaxation, dipolar interactions, and Au−SR binding sites (terraces, edges, vertexes).[23] The absence of sharp peaks in the ^{1}H NMR spectra demonstrated the effectiveness of the purification procedure in removing all nonligated thiols (including excess of incoming fluorenyl-alkane-1-thiol and displaced alkane-1-thiol).

The number of fluorophores present in the exchanged Au-MPC could then be calculated. With C_9S−Au-MPC, FlC_9SH replaced 100% of the protecting alkanethiol, whereas with $FlC_{12}SH$, 81% of the capping nonane-1-thiolate was displaced. For $C_{12}S$−Au-MPC, 84% and 62% exchanges, respectively, were obtained for FlC_9SH and $FlC_{12}SH$ as the entering thiols.

Thiolates bound to Au atoms lying at the interface between two flat faces are denoted as edge sites and those bound at the intersection of three flat faces are denoted as vertice sites. These sites have been proved to be the most easily exchanged.[22] Murray and co-workers have reported that ca. 4 of the most readily exchangeable sites are available on a 2.1-nm-diameter $Au_{314}(RS)_{108}$.[22]

The direct reduction of $AuCl_4^-$ with $NaBH_4$ in the presence of FlC_9SH produced particles that tended to aggregate in solution, whereas particles prepared by place exchange were dispersed evenly in the same medium (see Supporting Information). The difference was also clearly indicated by transmission FTIR and absorption spectroscopy.

Fourier Transform Infrared Spectra. To investigate the structure of fluorenyl-thiol-functionalized gold nanoparticles, transmission FTIR spectroscopy was carried out. Figure 2 shows the 4000−400-cm^{-1} region of the infrared spectra of a FlC_9S−Au-MPC, along with the spectra of C_9S−Au-MPC and of bulk FlC_9SH for comparison. It is clear that the synthetic material is a fluorene and gold composite.

The C−H stretching region has been used widely as a diagnostic of methylene chain ordering. All the alkane-1-thiolate Au-MPCs and the fluorenyl-alkane-1-thiolate Au-MPCs by place exchange show a crystalline microenvironment for the alkyl methylene groups, as clearly indicated by symmetric (d^+) and asymmetric (d^-) CH_2 stretching vibrations at 2849−2851 and 2919−2921 cm^{-1}. The methylene C−H stretching vibrations for pure FlC_9SH were found at 2852 and 2925 cm^{-1} and for pure $FlC_{12}SH$ at 2851 and 2923 cm^{-1}. The region of 1300−1400 cm^{-1} is rich in defect-related bands.[25] There are four wagging bands that can be assigned to defect structures: 1345 cm^{-1} for a chain end-gauche defect, 1366 and 1306 cm^{-1} for an internal kink defect, and 1353 cm^{-1} for a double gauche defect. In our spectra, there were weak peaks at 1345 and 1366 cm^{-1} and no double gauche defect. These spectra and thereby-deduced structured features are substantially preserved in the exchanged clusters.[5] The high density of the fluorenyl-alkane-1-thiols at the surface of fluorenyl-labeled Au-MPC allows for only a small number of gauche defects in the packed methylene chains.

The transmission FTIR showed the obvious difference between the gold clusters made by place exchange and by in situ capping. The sample prepared by direct reduction shows no clear peak at 3010−3070 cm^{-1} and a weak peak at 1449 cm^{-1}, which were assigned to the fluorenyl aromatic ═C−H stretch and ring C═C stretching bands, respectively. Thus, the gold clusters prepared by direct reduction in the presence of FlC_9SH produced only small yields of the desired clusters and instead produced insoluble higher aggregates.

Murray and co-workers have reported that gold clusters stabilized by monolayers of arenethiolates are larger and less thermally stable than those prepared under similar conditions and stabilized by the alkane-1-thiolates.[26] For example, PhS−Au-MPCs, synthesized at room temperature with a 100% molar excess of PhSH over gold, had an average diameter of 6.5 nm by TEM,

(25) Snyder, R. G. *J. Chem. Phys.* **1967**, *47*, 1316.
(26) Chen, S.; Murray, R. W. *Langmuir* **1999**, *15*, 682.

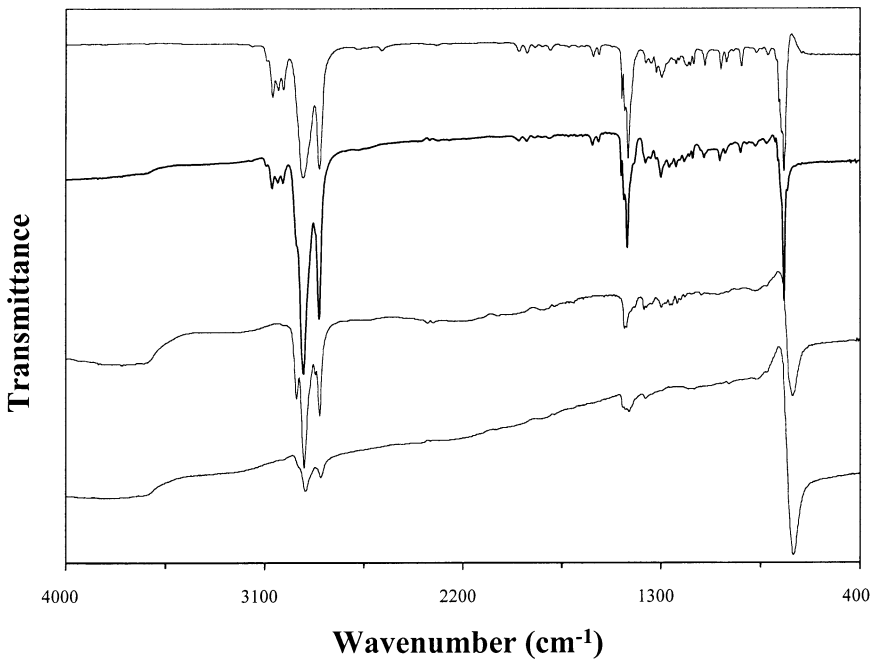

Figure 2. Transmission FTIR spectra of films (drop-cast on a KBr salt plate, from top to bottom) of FlC_9SH, FlC_9S−Au-MPC prepared by place exchange, C_9S−Au-MPC, and gold clusters prepared by direct reduction in the presence of FlC_9SH.

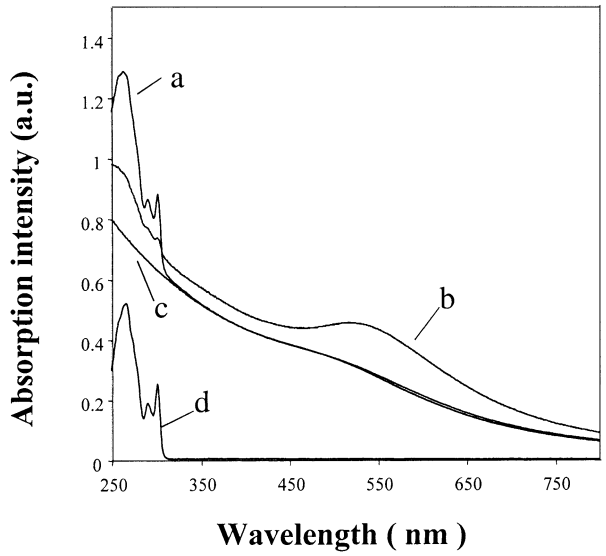

Figure 3. Absorption spectra of (a) FlC_9S−Au-MPC prepared by place exchange, (b) gold clusters prepared by direct reduction in the presence of FlC_9SH, (c) C_9S−Au-MPC, and (d) FlC_9SH (2.2×10^{-5} M) in dichloromethane.

whereas the alkane-1-thiolate MPCs synthesized at the same condition had an average diameter of about 2 nm.

Absorption Spectra. A broad weak absorption band around 530 nm arises from the surface plasmon absorption in the C_9S−Au-MPC (Figure 3). As indicated in earlier studies, the evolution of plasmon absorption as a prominent band is seen only for particles of diameter >5 nm.[27,28] Since TEM shows that the average size of C_9S−Au-MPC is about 2.2 nm, it is understandable that the surface plasmon band in these nanoparticles is very weak, indicated only by trailing absorption. FlC_9S−Au-MPC prepared by place exchange exhibits only a weak surface plasmon absorption as in C_9S−Au-MPC. The absorption spectrum of FlC_9S−Au-MPC shows three distinct bands (266, 290, and 302 nm) assigned to the absorptions by the fluorenyl group. FlC_9S−Au-MPC does not show any new peaks: the observed spectrum is the simple sum of the spectrum expected for homogeneously dispersed fluorenyl thiol and C_9S−Au-MPC. Because C_9S−Au-MPC and FlC_9S−Au-MPC have identical surface plasmon absorptions, the metallic core must retain its original size upon place exchange. Specifically, a broad well-defined absorption band around 530 nm arises from the surface plasmon absorption in the gold clusters prepared by in situ capping. Also, the UV region shows very weak absorption from the fluorenyl moieties.

Thus, the fluorenyl-alkane-1-thiolate Au-MPCs prepared by place exchange have a shell−core structure in which methylene groups of the alkyl chains are densely packed. In contrast, direct reduction of $HAuCl_4$ in the presence of FlC_9SH failed to produce monodispersed gold clusters.

Steady-State Fluorescence Spectra. The emission spectrum of FlC_9SH as a homogeneous solution in dichloromethane shows a maximum at 313 nm. The emission spectra of the fluorenyl-alkane-1-thiolate Au-MPCs retained this same shape and peak position, but the intensity of emission was strongly quenched. This result is different from the fluorescence of fluorenyl-alkane-1-thiols as SAMs on planar gold, where the surface fluorescence maxima were red-shifted and the band broadened compared with the corresponding spectral features measured in dilute solution.[29]

In principle, the observed quenching could be caused by either decreased absorption by the appended fluorene in competition with the gold core or deactivation by the gold core. To separate these effects, we prepared a

(27) Alvarez, M. M.; Khoury, J. T.; Schaaff, T. G.; Shafigullin, M. N.; Vezmar, I.; Whetten, R. L. *J. Phys. Chem. B* **1997**, *101*, 3706.
(28) Henglein, A. *Langmuir* **1998**, *14*, 6738.
(29) Kittredge, K. W., Fox, M. A., Whitesell, J. K. *J. Phys. Chem. B* **2001**, *105*, 10594.

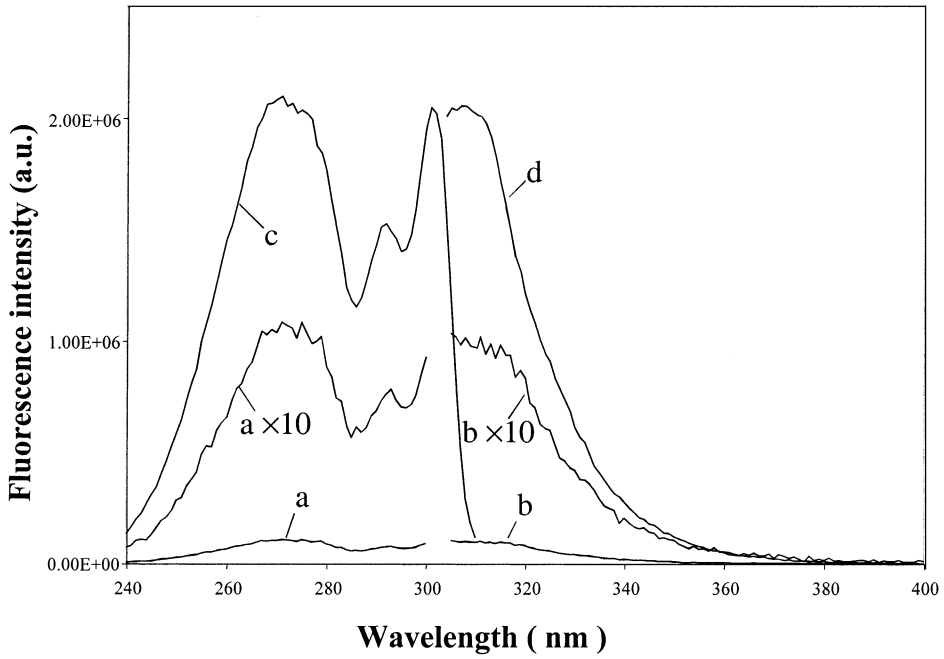

Figure 4. Excitation and emission spectra of FlC_9S−Au-MPC (a and b) and the corresponding spectra form an optically matched mixture of FlC_9SH and C_9S−Au-MPC (c and d) in CH_2Cl_2. Excitation wavelength is 266 nm and emission wavelength is 313 nm. The optical density of the solution at 266 nm is about 0.5.

solution-phase mixture of alkane-1-thiolate Au-MPCs and fluorenyl-alkane-1-thiol, which is optically matched to a fluorenyl-alkane-1-thiolate Au-MPC solution. (This mixture solution prepared just before the fluorescence emission experiment is not complicated by the slower place-exchange reaction where the reaction is driven by a large excess of fluorenyl thiol.) The excitation and emission spectra of FlC_9S−Au-MPC, Figure 4, curves a and b, are identical in shape and wavelength maxima to those shown in curves c and d, the optically matched solution of unattached FlC_9SH and C_9S−Au-MPC. The principal difference between two samples is that the fluorescence emission of FlC_9S−Au-MPC is strongly quenched compared with the corresponding optically matched solution. (The fluorescence intensity of the former is only about 5% of that of the latter). Thus, the intensity difference results from the attachment of the fluorenyl probe to the core gold cluster, rather than from competitive absorption by the gold monolayer-protected cluster.

Differential loading of the emissive fluorenyl groups on the gold cluster also affected the magnitude of the observed emission quenching. The emission yield (compared to the optically matched solution of FlC_9SH and C_9S−Au-MPC) is 5.0%, 2.4%, and 1.4% of the corresponding fluorenyl-capped gold clusters with 100%, 71%, and 48% fluorenyl loading, respectively. Efficient energy transfer can explain reasonably these observations. High loading levels would suppress folding of the alkyl linker so that, with an extended chain, reduced distance-dependent electronic coupling, and hence reduced energy-transfer efficiency, would be expected. Murray and coworkers have shown that the emission intensity per MPC-attached dansyl group increases with surface loading and with the length of the connecting linker chain.[13]

Nanosecond Flash Photolysis. In principle, the observed fluorescence quenching could result from enhanced intersystem crossing efficiency, from energy transfer to the gold core, or from photoinduced electron transfer from the excited fluorenyl group to the gold core. To differentiate these possible deactivation pathways, transient absorption kinetics following a 266-nm laser excitation pulse were monitored.

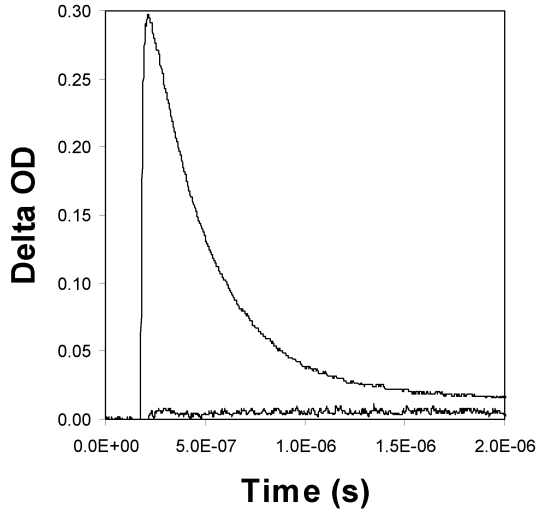

Figure 5. Absorption decay profiles of FlC_9SH (top) and FlC_9S−Au-MPCs (bottom) in CH_2Cl_2 with N_2 bubbling recorded at 380 nm upon 266-nm pulse excitation. The optical density of the solution at 266 nm is about 0.5.

A transient observed from pulse excitation of free FlC_9SH (Figure 5) followed monoexponential decay kinetics with a lifetime of 0.3 μs, as expected for a triplet−triplet absorption. This lifetime is shorter than reported data[30] collected in degassed solution since oxygen strongly quenches the triplet. Because gold clusters contribute to the net absorption at 266 nm, the

(30) Murov, S. L.; Carmichael, I.; Hug, G. L. *Handbook of Photochemistry*, 2nd ed.; Marcel Dekker: New York, 1993; p 113.

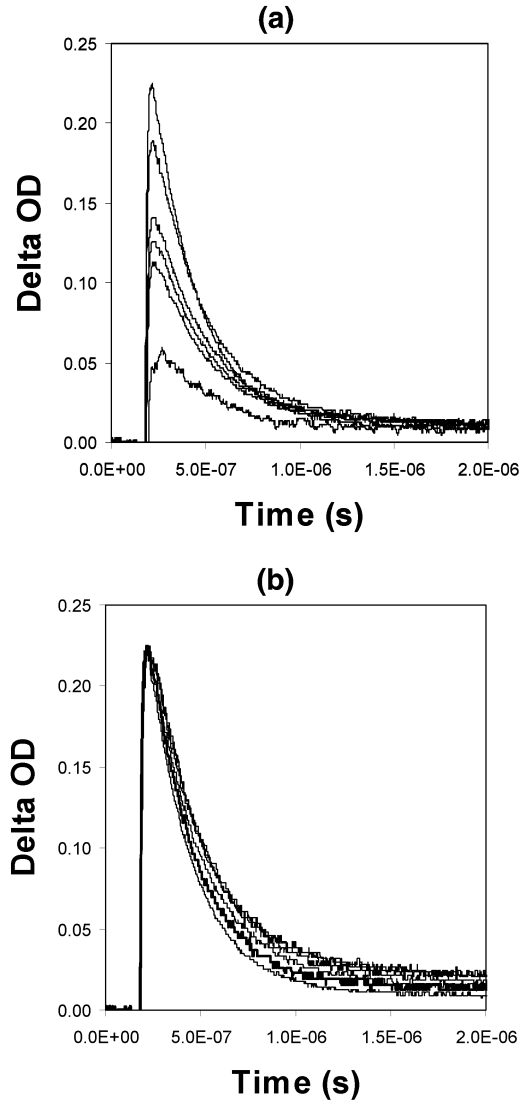

Figure 6. (a) The absorption decay profiles of FlC_9SH (the optical density at 266 nm is about 0.5) and a mixture with the addition of C_9S−Au-MPC (from top to bottom, the concentration of C_9S−Au-MPC is increased) in CH_2Cl_2 recorded at 380 nm upon 266-nm pulse excitation with N_2 bubbling. (b) Normalization of the transient decay in Figure 6a.

transient absorption spectrum of C_9S−Au-MPC was also recorded. No transient absorption signal was observed at the probe wavelength (380 nm) upon excitation at 266 nm, with or without deaeration by nitrogen bubbling. Transient signals observed with FlC_9S−Au-MPC at 380 nm upon excitation at 266 nm, with and without nitrogen bubbling, produced no evidence for triplet−triplet absorption. Compared with the free FlC_9SH's lifetime of 0.3 μs, a substantial decrease of both transient intensity and lifetime of the fluorophore attached to the gold nanocore was observed. Further information about the decreased lifetime of FlC_9SH chemically attached to the gold nanoparticle proved to be elusive because the time resolution of nanosecond flash photolysis equipment is more than 10 ns.

The transient absorption from a fresh mixture of C_9S−Au-MPC and FlC_9SH was also measured. The decay curve of the transient absorption signal at 380 nm is similar to that of FlC_9SH (Figure 6a). With the addition of C_9S−Au-MPC, the transient signal intensity became weak. Upon normalization of the transient decay at different C_9S−Au-MPC concentrations, the same transient decay kinetics as free FlC_9SH were recorded with a lifetime of 0.3 μs (Figure 6b), indicating that the excited fluorenyl triplet was quenched via static quenching when mixing C_9S−Au-MPC with unattached FlC_9SH.

Differences between the transient absorptions of FlC_9S−Au-MPC and the optically matched mixture of C_9S−Au-MPC and unattached FlC_9SH indicate that intersystem crossing of the excited fluorenyl singlet to the triplet is suppressed when bound to the gold nanoparticle. If intersystem crossing is not the main deactivating pathway for the observed strong fluorene emission quenching in FlC_9S−Au-MPC, then electron or/and energy transfer are likely dominant pathways.

To explore the possibility of deactivation by electron transfer, a solution of FlC_9S−Au-MPC was probed at 350, 400, and 660 nm. These regions were chosen because the fluorenyl anion radical has been reported to absorb at 375−400 and 650−707 nm and the fluorenyl cation radical at 355−378 and 610−663 nm.[31] No transient anion radical or cation radical absorption signal could be observed at any of the above probe wavelengths. This excludes the possibility that the fluorescence emission quenching in the fluorenyl-capped gold clusters takes place primarily via electron transfer.

If electron transfer is not a major deactivation pathway for FlC_9S−Au-MPC, then the low yields of both the singlet and triplet confirm that the excitation energy is quickly deactivated through electronic coupling of the excited fluorenyl group with the gold cluster.

Conclusion

Fluorenyl-alkane-1-thiolate Au-MPCs were prepared by place exchange of an alkane-1-thiolate-protected gold cluster. The structures of these composites were established by spectroscopy including TEM, ^{1}H NMR, absorption, and transmission FTIR measurements. FlC_9SH−Au-MPCs prepared by place exchange have a shell−core structure in which methylene groups of the alkyl chains are densely packed. Direct borohydride reduction of $HAuCl_4$ in the presence of FlC_9SH fails to produce monodispersed gold clusters. The strong fluorescence emission quenching of the fluorenyl-alkane-1-thiolate Au-MPCs compared to the optically matched solution of homogeneously dispersed fluorenyl thiol and alkane-1-thiolate Au-MPCs was attributed to the covalent attachment of the fluorenyl probe to the gold clusters, thus facilitating strong through-bond electronic coupling. Nanosecond flash photolysis shows that intersystem crossing from the excited fluorenyl singlet to the corresponding triplet was suppressed, implying that deactivation by the gold cluster is much faster than intersystem crossing. And the possibility of electron transfer between the excited fluorene singlet and gold clusters was excluded because no fluorenyl radical, radical cation, or radical anion transient could be observed. The strong quenching of fluorescence emission, as well as deeply decreased yields of triplet, imply energy transfer as the principle mode for electronic

(31) Shida, T. *Electronic Absorption Spectra of Radical Ions*; Elsevier: Amsterdam, 1988; p 137.

coupling between the excited fluorenyl group and the included gold clusters.

Acknowledgment. This work was supported by the U.S. Department of Energy. The authors gratefully acknowledge Dr. Yuri V. Il'ichev and Dr. John D. Simon of Duke University for assistance with the nanosecond flash photolysis experiments.

Supporting Information Available: TEM images of FlC_9S−Au-MPC prepared by place exchange (Figure S1) and in situ direct reduction of $AuCl_4^-$ with $NaBH_4$ in the presence of FlC_9SH (Figure S2), ^1H NMR spectra of fluorenyl-alkane-1-thiolate Au-MPCs (Figures S3, S4, S5, S6, S7, and S8) (PDF). This material is available free of charge via the Internet at http://pubs.acs.org.

CM0209867